Cell

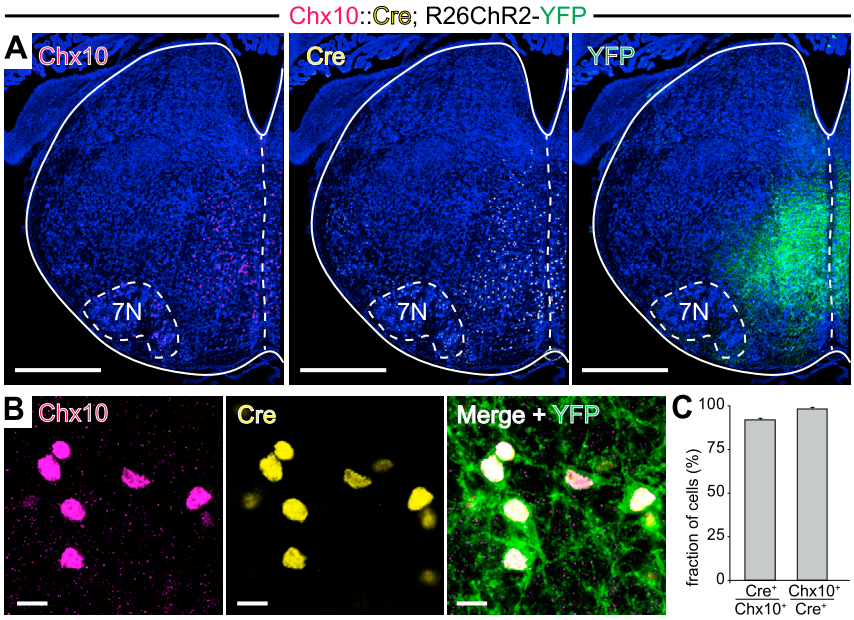

Figure S1. *Chx10::Cre* Line Reliably Drives Cre Expression and Flox-Mediated Recombination in Chx10$^+$ Cells, Related to Figures 1, 2, 3, 4, 5, 6, 7

(A) Confocal maximum projection picture of a 20 μm-thick transverse hemisection (left-side is depicted) at the level of the rGi area of a *Chx10::Cre; R26ChR2-YFP* newborn animal stained with a fluorescent Nissl (blue) and against Chx10 (magenta, left), Cre (yellow, middle), and YFP (green, right). Note the overlapping expression of Chx10, Cre, and YFP.

(B) Higher magnification of a single z-plane within the rGi showing that Chx10$^+$; Cre$^+$ nuclei are surrounded by YFP cytoplasmic expression.

(C) Bar-graph illustrating the average percentage (n = 3 animals) of Cre$^+$ cells that co-express Chx10 (92% ± 0.8%) and of Chx10$^+$ cells that co-express Cre (99% ± 0.8%). Error bars are SEM.

Scale bars, 500 μm (A); 10 μm (B).

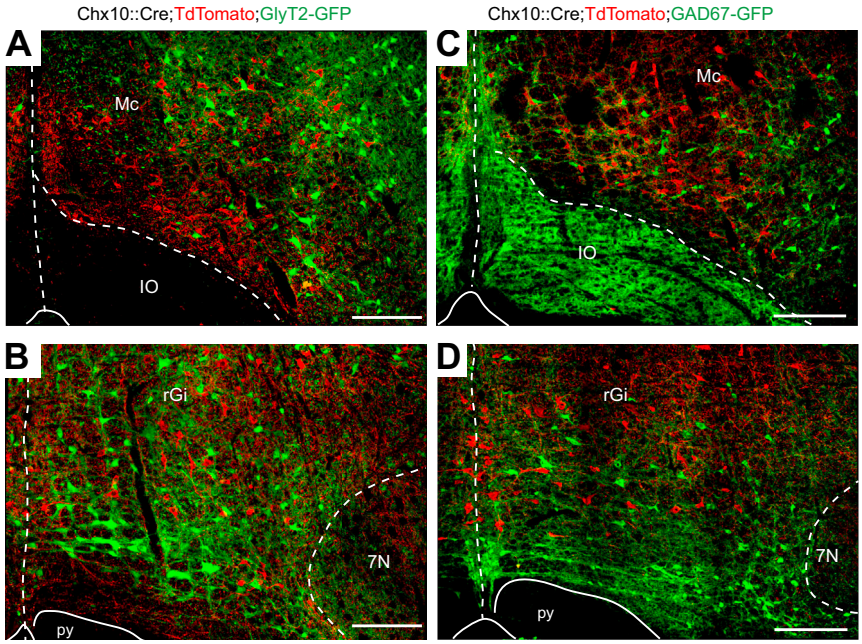

Figure S2. Medullary V2a Neurons Do Not Co-express Inhibitory Markers, Related to Figure 1

(A, B) Confocal maximum projections of 20 μm-thick transverse brainstem hemi-sections of a *Chx10::Cre; Tdtomato; GlyT2-GFP* animal at two representative rostro-caudal levels (see Figure 1): that of the Mc caudally (A) and of the rGi rostrally (B). Tdtomato (red) reports V2a neurons, while GFP (green) reports the expression of the glycine transporter and reveals glycinergic neurons (Restrepo et al., 2009; Zeilhofer et al., 2005). Note the rare overlap (PnC: 5/164 cells, 3%; rGi: 8/258, 3%; cGi: 3/242, 1%; Mc: 2/232, < 1%, n = 2 animals)

(C, D) Similar representations obtained on a *Chx10::Cre;Tdtomato; GAD67-GFP* animal where GFP (green) now reports the expression of the Glutamic Acid Decarboxylase (isoform 67, GAD67; Restrepo et al., 2009) that synthesizes the inhibitory amino acid GABA and thus reveals GABAergic neurons. Note the rare overlap (PnC: 3/347 cells, < 1%; rGi: 2/547, < 1%; cGi: 4/433, < 1%; Mc: 6/406, 1.5%, n = 3 animals) neurons. Scale bars, 200 μm.

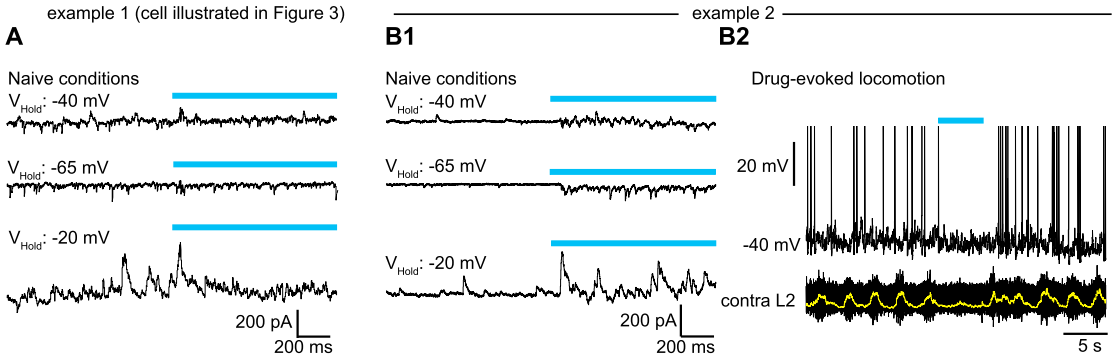

Figure S3. Synaptic Responses in Lumbar Motor Neurons Evoked by Optogenetic Activation of Brainstem V2a Neurons in the Absence of Locomotor-like Activity, Related to Figure 3

(A) Same lumbar motor neuron as illustrated in Figure 3B, recorded in voltage-clamp in the absence of locomotor drugs in the spinal compartment and in the presence of KYN in the brainstem and supra-lumbar segments. In this cell, light-activation of brainstem V2a neurons (blue bar) evokes no significant changes in excitatory and inhibitory post-synaptic currents (EPSC and IPSC, respectively) frequency ($p > 0.5$, paired t test) in the motor neuron held at −20, −40, or −65 mV. (B) Recordings of another motor neuron that shows a significant increase in the frequency of both EPSCs and IPSCs (B1) upon light-activation of brainstem V2a neurons. At intermediate holding potentials (−40 mV, top trace) light-activation of brainstem V2a neurons evokes a mixture of EPSC and IPSC. Holding the cell at −65 mV (middle trace) isolates excitatory currents while inhibitory ones are more clearly distinguishable at −20 mV (bottom trace). During drug-evoked locomotion, this cell shows rhythmic firing and is silenced upon brainstem V2a neuron activation (B2).

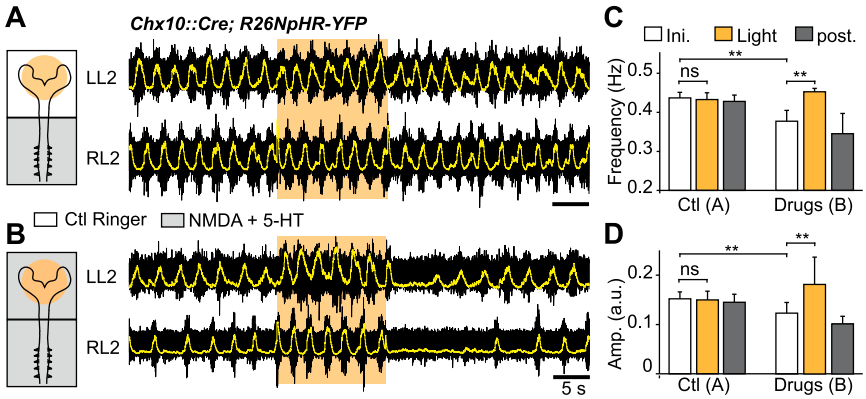

Figure S4. Optogenetic Inhibition of V2a Brainstem Neurons During Locomotor-like Activity, Related to Figure 3

(A, B) Left: schematic representations of the spilt-bath configuration allowing locomotor drugs (NMDA and 5-HT) to be bath-applied over the lumbar spinal cord only (A), or over both the brainstem and spinal cord (B). The yellow circle illustrates the area where light is delivered continuously through the 5× microscope objective.

(C, D) Average frequency (C) and percent change in amplitude (D) before (white box), during (yellow box), and for the five first cycles after (dark gray box) light-inhibition of brainstem V2a neurons (n = 3 animals). When the locomotor-like activity was induced by applying neuroactive drugs selectively over the lumbar spinal cord, light stimulation (continuous illumination for 5–10 s, 536–576 nm) of V2a brainstem neurons did not significantly alter the ongoing locomotor frequency (A, C). In contrast when neuroactive drugs were also applied onto the brainstem, the frequency of the drug-induced lumbar locomotor-like activity decreased (86% ± 5% of control). Under these conditions light-inhibition of V2a brainstem neurons now caused a significant increase in the lumbar locomotor-like frequency (121% ± 10% of control; B, C) and amplitude (142% ± 24% of control; B, D). Light-offset was followed by a short period of reduced activity, which may owe to a post-inhibitory rebound activity in illuminated V2a neurons, thus allowing the transient manifestation of their locomotor "stop" effect upon termination of the light stimulation. Such rebound effects following light stimulation with halorhodopsin are well-known in the motor system (Arrenberg et al., 2009; Warp et al., 2012). Ns indicates non-significant ($p > 0.05$), ** indicates $p < 0.01$ (paired t test).

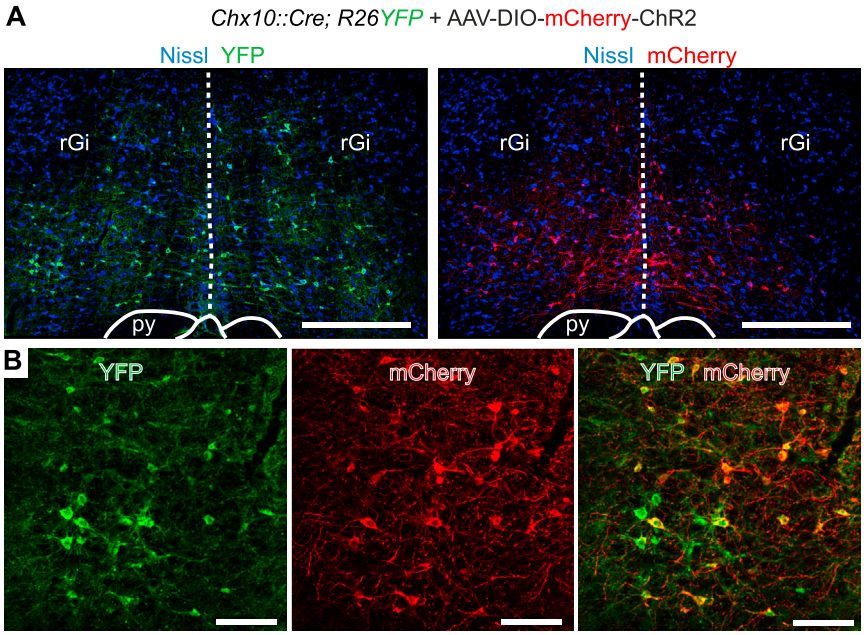

Figure S5. Selective Viral Transfection of V2a Neurons, Related to Figures 5 and 7

(A) Confocal maximum projection picture of a 30 μm-thick transverse section at the level of the rGi area of a *Chx10::Cre; R26ChR2-YFP* adult mouse showing V2a (YFP, green) and virally transfected (mCherry, Red) neurons on a Nissl background (Blue), 6 weeks following the bilateral injection of the Cre-dependent AAV-DIO-mCherry-ChR2 virus. The dashed line depicts the midline.

(B) Higher magnification within the rGi showing that virally driven mCherry expression is restricted to V2a neurons. Scale bars, 500 μm (A); 100 μm (B).

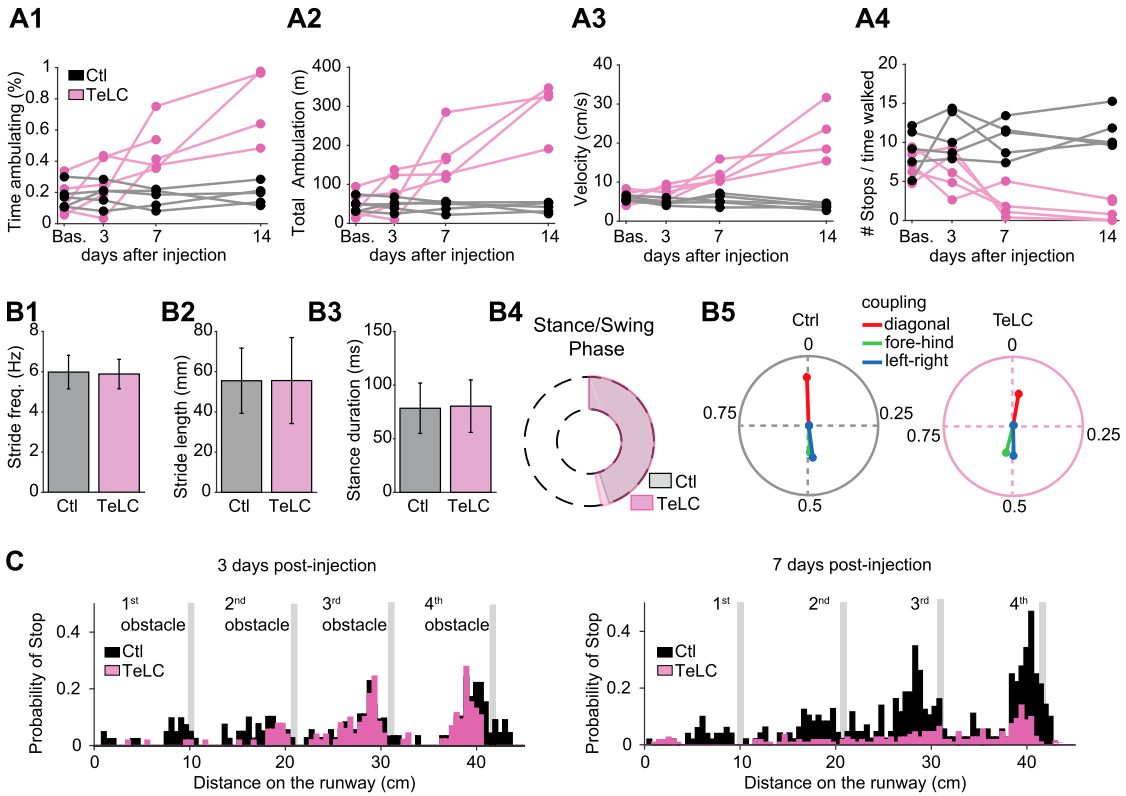

Figure S6. Effects on Locomotion and Ability to Stop by Genetic Silencing of V2a Neurons, Related to Figure 6.

(A1–A4) Development of ambulation, total length of ambulation, velocity and stop events in the open field test for individual saline-injected (black, n = 5) and TeLC-treated (pink, n = 5) animals before ('bas.'), and at 3, 7, and 9 days after the injection.

(A1) Normalized time spending ambulating.

(A2) Total distance achieved while ambulating (m).

(A3) Velocity of ambulation (cm/s).

(A4) Number of stop events per time spent ambulating.

(B1–B5) Kinematic gait analysis of saline-injected (n = 5, gray) and TeLC-treated (n = 5, pink) animals moving on a treadmill at similar frequencies (5–9 Hz; 402 steps saline injected and 326 steps TeLC-treated). Bar plots indicate average and SD. There were no differences (calculated with U test statistics) in stride frequency (B1; $p > 0.05$), stride length (B2; $p > 0.05$), stance duration (B3; $p > 0.05$), or relative duration of stance/swing phase (B4; $p > 0.05$). The most common gait was trot as shown by the four-limb coupling: left-right and ipsilateral fore-limb/hindlimb phase coupling around 0.5 and diagonal fore-limb/hindlimb coupling around 1.0 (see Bellardita and Kiehn 2015). No difference between treatments was observed (B5; $p > 0.05$, U-Test for circular data). This indicates that gait patterns are normal in mice where synaptic transmission is blocked in V2a stop neurons by TeLC toxins.

(C) Histograms showing the probability of stop events for saline-injected (n = 6) or TeLC-treated (n = 8) mice, 3 and 7 days after injections.

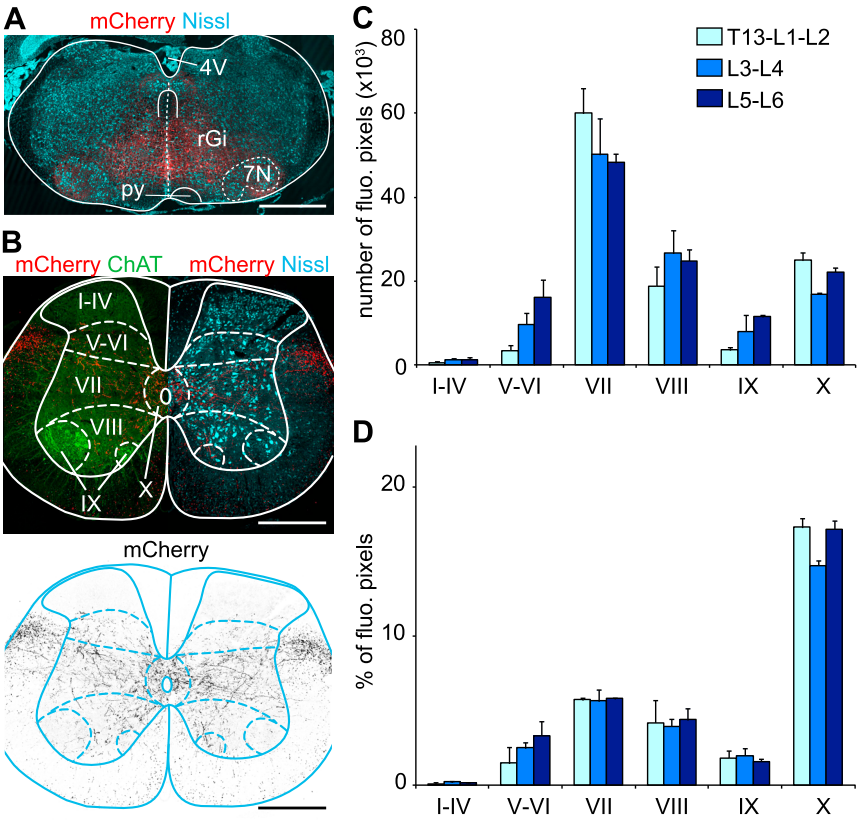

Figure S7. V2a Stop Neurons Terminate Predominantly in Lamina VII of the Lumbar Spinal Cord, Related to Figure 7

(A) Anterograde labeling approach as described in Figure 7, illustrated here on another animal. After a recovery time of 6 weeks post-injection, mCherry-transfected cells are visualized on 20 μm-thick transverse sections stained with an anti-RFP antibody on top of a fluorescent Nissl background (cyan).

(B) Confocal picture of a 14 μm-thick transverse section at the L2 level of the spinal cord of the same animal. A co-labeling with a ChAT antibody (green, top left hemi-cord) and a fluorescent Nissl (cyan, top right hemi-cord) is used to delineate the Rexed's laminae (dashed lines) while the RFP antibody (red on top, black on bottom) labels the transfected V2a neuronal processes.

(C–D) Quantification of the number of fluorescent pixels (C) or the fraction of fluorescent pixels per area (in percent; D) in each lamina indicated in (B) at the upper (T13-L1-L2), intermediate (L3-L4), and caudal (L5-L6) lumbar levels for the illustrated example. A comparable innervation pattern was observed on one additional animal, albeit absolute numbers differed and is thus depicted on Figure 7.

Scale bars (in μm): 1,000 (A); 500 (B).

Cell

Supplemental Information

Descending Command Neurons in the Brainstem that Halt Locomotion

Julien Bouvier, Vittorio Caggiano, Roberto Leiras, Vanessa Caldeira, Carmelo Bellardita, Kira Balueva, Andrea Fuchs, and Ole Kiehn

SUPPLEMENTAL EXPERIMENTAL PROCEDURES

Retrograde labeling of reticulospinal neurons

Chx10::Cre mice were crossed with a conditional reporter line (*Rosa26*^{FlxYFP} or *Rosa26*^{FlxTdtomato}) and occasionally with an additional straight reporter line (*GlyT2-GFP* or *GAD67-GFP*). Appropriate crosses, aged 1-2 months, were anesthetized with isoflurane and shaved on the dorsal side. A two cm incision of the skin was performed dorsally and the exposed spinal column was fixed with two holders on the left and right sides to prevent movements. Vertebral spinous processes were used as landmarks to target specific segments (Harrison et al., 2013). A small incision of the ligamentum Flavum allowed access to the spinal cord without performing a laminectomy. A glass pipette, connected to a motorized pressure injector (Quintessential Sterotaxic Injection, Stoelting, Wood Dale, IL) was positioned onto the spinal cord, 300 µm laterally from the dorsal artery and lowered to 900 µm from the dorsal surface. A total volume of 0.5 to 0.75 µL of CTB (0.5 % in saline, List Biological Laboratories) was injected at 100 nL/min onto each sides of the lumbar spinal cord. During the injection, the pipette was retracted to 500 µm and lowered up to 1200 µm from the dorsal surface to favor a greater spread. The pipette was held in place for 5 min following the injection before being slowly retracted, and the procedure was repeated on the other side of the cord. The skin was sutured, and analgesics (Buprenorphin, 0.01 mg/kg) were given post-surgery.

Neurotransmitter phenotyping and immunohistochemical stainings

Adult animals were anesthetized with pentobarbital and perfused with 4 % (wg/vol) paraformaldehyde in Phosphate-Buffered-Saline (PBS). Brains and spinal cord were dissected out and post-fixed overnight in 4 % PFA. For postnatal tissue collection, pups aged 0-4 days were anesthetized in isoflurane, decerebrated and eviscerated and the brainstem was isolated and fixed in 4 % PFA at 4 °C for 1-3 hours. After fixation, tissues were rinsed in PBS, cryoprotected in 20 % (wg/vol) sucrose in PBS overnight and rapidly cryo-embedded in OCT mounting medium. Transverse sections (14-30 µm-thick) were obtained on a cryostat. Sections were blocked in Tris-Buffered Saline (TBS) supplemented with 5 % (vol/vol) Normal Donkey Serum (Jackson Immunoresearch) and 0.5 % (wg/vol) Triton X-100 before being incubated 24 to 48 hours at 4° C with one or several of the following primary antibodies: goat anti-CTB (1:1000,

List Biological Laboratories #703), rabbit anti-RFP (1:1000, Rockland 600-401-379), chicken anti-GFP (1:1000, Aves Labs 1020), goat anti-ChAT (1:200, Millipore AB144P), mouse anti-TPH (1:2000, Millipore MAB5278), rabbit anti-Cre (1:8000, kind gift from Dr. G. Shutz), sheep anti-Chx10 (1:300, Millipore AB9016). Secondary antibodies [F(ab')$_2$fragments] were obtained from Jackson Immunoresearch or Invitrogen, used at 1:400 and incubated for 3 h at room temperature. When applicable, a fluorescent Nissl stain (NeuroTrace Blue 1:200, or NeuroTrace Deep Red 1:1000, Life Technologies) was added during the secondary antibody incubation. Slides were rinsed, mounted in Prolong diamond antifade mountant (Life Technologies) and scanned on a LSM510 confocal microscope (Zeiss Microsystems) using 10x, 20x and 40x objectives. Multiple channels were scanned sequentially to prevent fluorescence bleed through and false-positive signals. A contrast enhancement and a noise reduction filter were applied in Adobe Photoshop for publication images. Fluorescent *in situ* hybridization combined with immunofluorescence labeling was performed as previously described (Borgius et al., 2010) using a Vglut2 probe spanning the base pairs 540–983 (produced by Dr. L. Borgius).

Anatomical delineations of brainstem structures and cellular counts

Brainstem areas were delineated by systematically performing a Nissl stain on experimental sections when possible, or alternatively on a dedicated set of sections. The relative distance to Bregma was established by comparing the Nissl stain with that of the Mouse Brain atlas by (Paxinos and Franklin, 2001). We used the following criteria to reproducibly allocate labeled neurons to a precise brainstem structure, from caudal to rostral. Retrogradely-labeled neurons located medially (0-1 mm from the midline) were considered as part of: the magnocellular nuclei (Mc) from the rostral edge of the pyramidal decussation caudally, to the opening of the 4th ventricle (obex) rostrally (from approximately -8.0 to -7.3 from Bregma); the gigantocellularis (Gi) nucleus and its ventral part (thereafter named caudal Gigantocellularis, cGi) between the obex caudally, and the caudal edge of the facial motor nucleus (7N, approximately -6.5 from Bregma) rostrally; the Gi nucleus and its alpha part (thereafter named rostral Gigantocellularis, rGi) from the caudal edge of the 7N caudally, to the caudal edge of the superior olivary complex (SOC) rostrally (approximately -5.6 from Bregma); the caudal pontine reticular nucleus (PnC) from caudal edge of the SOC to the motor trigeminal nucleus (Mo5) rostrally (approximately -5.0 from Bregma).

For each marker combination, neurons were counted on the same side, using raw z-stack confocal images obtained with a 20x or 40x objective and spanning the entire thickness of the sections. Counts were done manually with the help of the cell-counter plug-in in ImageJ, in 2-4 non-adjacent sections per mice (3-4) in each condition. Cellular counts per hemisection were averaged (or expressed as percentage) per individual animal, and a grand-mean ± standard error of the mean (SEM) was calculated across animals to produce cell per hemisection bar-graphs.

In vitro recording of locomotor activity

Mice aged 0-4 days were used in all experiments. The pups were anesthetized in isoflurane, decerebrated above the ponto-medullary junction (thus leaving the caudal pontine reticular nucleus the rostral-most preserved structure) and eviscerated. The spinal cord and brainstem were isolated in ice-cold low calcium Ringers solution (oxygenated in 95 % O_2 and 5 % CO_2) that contained in mM: 111 NaCl, 3 KCl, 11 glucose, 25 $NaHCO_3$, 3.7 $MgSO_4$, 1.1 KH_2PO_4, 0.25 $CaCl_2$ (pH: 7.4). V2a reticulospinal neurons being located below the ventral surface, their exposure to incident light was favored by performing an open book preparation. For this, the dura matter surrounding the brainstem was removed with fine forceps, and a longitudinal cut spanning the entire thickness of the preparation was performed along the midline from the rostral edge of the preparation to the pyramidal decussation, with a fine scalpel. The preparation was "opened" by tilting each hemi-brainstem ~45° laterally and stabilized by pinning down the rostral-most lateral edges of the caudal pons on a Sylgard surface. The preparation was transferred to a recording chamber that was continuously superfused with normal Ringers solution that contained in mM: 111 NaCl, 3 KCl, 11 glucose, 25 $NaHCO_3$, 1.25 $MgSO_4$, 1.1 KH_2PO_4, 2.5 $CaCl_2$ oxygenated in 95 % O_2 and 5 % CO_2 to obtain a pH of 7.4. All recordings were done at room temperature. The locomotor activity was recorded with suction electrodes attached to the L2 and/or the L5 lumbar roots. The ventral root activity was band-passed filtered at 100 Hz to 1 kHz and integrated with a time constant of 200 ms. Signals were sampled using Clampex 10 (Molecular Devices) at 1-2 kHz. To obtain separate perfusions of the brainstem and the spinal cord we used a split-bath configuration consisting of a Vaseline barrier placed over the T8-T12 segments. The integrity of the barrier was examined after the experiment by perfusing one of the compartments with Fast-Green and visually inspecting that there was no leakage.

Optogenetic stimulations *in vitro*

Light from a 100W Hg lamp was filtered by a 450-490 nm band-pass filter for ChR2 or a 536-556 nm band-pass filter for eNpHR, and was directed onto the preparation through a 5x objective. The intensity of the light was estimated to be about 32 mW mm^{-2} without light neutralization filters (see Hagglund et al., 2010).

Analysis of *in vitro* locomotor data

Changes in instantaneous locomotor frequencies were measured using the event detection tool in Clampfit 10 for each trial, defined as: a 20 sec period prior to light activation (initial), during continuous light activation (light), for the first 5 cycles following light offset (post-light), and for another 20 seconds (recovery). Two to 4 trials were considered for each preparation. Statistical significance between relevant conditions among all trials was tested using paired Student's t-test and values were considered as statistically different when $p < 0.05$.

Flexor-extensor and left-right coordination were evaluated for each trial – i.e. before and during light-activation - with circular statistics (see Kjaerulff and Kiehn, 1996), in which the vector direction gives the preferred phase of the activity and the length of the vector (r) the precision of the phase. p values larger than 0.05 determined by Rayleigh's test were considered non-significant. Values of phases were expressed in mean angles and angular dispersion. The Watson-Williams test for two samples was used to compare coordination at different conditions in the same preparation or condition in animals.

Drug-induced and neuronally-induced locomotor-like activities

Drug-evoked locomotor-like activity was induced by a combination of N-methyl-D-aspartate (NMDA, Tocris) and serotonin (5-HT; Sigma). To block glutamatergic transmission, we applied the broad spectrum non-NMDA and NMDA receptor blocker kynurenic acid (KYN, 4 mM, Sigma), selectively in the brainstem compartment in the split-bath configuration. Neuronally-evoked locomotor-like activity was elicited by electrical stimulation of the midline in upper cervical segments (0.5-2 mA amplitude, 10 ms duration, and 0.5-1 Hz frequencies) through a glass pipette electrode.

Motor neuron recordings

Motor neurons were identified visually after two hours retrograde transport of Tetramethyl-Rhodamine Dextran (3000 MW), using a FITC filter-set and differential interference contrast. Patch electrodes were obtained from filamented borosilicate glass tube (GC 150F) and filled with a solution containing (in mM): 128 K-gluconate, 10 HEPES, 0.0001 $CaCl_2$, 1 glucose, 4 NaCl, 5 ATP, 0.3 GTP, pH 7.4. When filled with this solution the pipette resistance was 3-6 MΩ. The calculated reversal potential for IPSPs with this pipette solution and standard extracellular Ringers solution is approximately -85 mV. Whole-cell recordings were performed at room temperature using a Multiclamp 700B amplifier (Molecular Devices) and acquired using pClamp software (Clampex v.10, Molecular Devices). Membrane potentials were not corrected for the liquid junction potential induced by whole-cell configuration (approximately 10 mV).

***In vivo* optogenetic experiments**

Viral injections and ferrule implantation. A total of 600 nL of an AAVDj-EF1a-DIO-hChR2-p2A-mCheery-WRPE (titer 9.10e12 particles/mL) was injected by a glass micropipette using a Quintessential Sterotaxic Injector (Stoelting, Wood Dale, IL), in the rostral gigantocellularis nucleus bilaterally (6.0 mm caudal to Bregma, 0.5 mm Lateral, 4.0 mm from dorsal surface) at 100 nL/min. Following the injection, the pipette was held in place for 5 min before being slowly retracted. In the same surgery, an optical fiber (200 μm core, 0.22 NA, Thorlabs) held in a 1.25 mm ferrule was implanted at the midline (depth -3.5 mm from dorsal surface) to ensure bilateral stimulation of the transfected cells. The ferrule was chronically kept in place by applying light curing dental cement. Mice were allowed 3-4 weeks for recovery before being challenged to behavioral experiments. Analgesics (Buprenorphin, 0.03 mg/kg) were given after the surgery and once a day for 4 consecutive days post-surgery. For selective blocking synaptic output of V2a stop neurons, 300 to 700 nL of an AAV-FLEX-TeLC virus was injected bilaterally in the rGi.

Evaluation of firing in ChR2 infected brainstem neurons. To evaluate that ChR2 expressing cells in the brainstem responded to light we harvested tissue from adult mice that had been injected with the virus 4 weeks before**.** Brainstem slices for patch clamp recording were prepared as previously described (Fuchs et al., 2013). Briefly, mice were anesthetized with

ketamine/medetomidine hydrochloride (250 mg/kg and 2.5 mg/kg, respectively) and intracardially perfused with ice-cold artificial cerebrospinal fluid (perfusion ACSF: in mM: 125 NaCl, 2.5 KCl, 25 $NaHCO_3$, 1.25 NaH_2PO_4, 2.5 glucose, 50 sucrose, 0.1 $CaCl_2$, 6 $MgCl_2$, 3 kynurenic acid, oxygenated with 95 % O_2, 5 % CO_2). Perfused mice were decapitated and the brain was quickly removed from the skull. Brains were glued on a specimen holder and coronal slices (250 µm) were cut in 4 °C bubbled perfusion ACSF using a vibratome (HM650V, Thermo Scientific – Microm). Slices recovered for 90 min at 36 °C in bubbled recording ACSF (in mM: 125 NaCl, 2.5 KCl, 25 $NaHCO_3$, 1.25 NaH_2PO_4, 2.5 glucose, 22.5 sucrose, 2 $CaCl_2$, 2 $MgCl_2$, oxygenated with 95 % O_2, 5% CO_2) and kept at room temperature until transfer to the bath chamber. Slices were superfused with oxygenated recording ACSF. Ten µM CNQX, 20 µM AP5, 20 µM Picrotoxin and 0.5 µM Strychnine were added to block all synaptic inputs. Experiments were performed at room temperature. Patch pipettes (5-6 MΩ) were pulled from borosilicate glass (GC150F-10, Harvard Apparatus) and filled with (in mM): 128 KGlu, 4 NaCl, 10 HEPES, 0.0001 $CaCl_2$, 1 glucose, 5 ATP, 0.3 GTP, pH 7.4. Neurons were visualized by video microscopy (Axioskop 2 FS plus, Zeiss) using transversal illumination for increasing contrast and virus-infected Chx10 neurons were identified under fluorescence using a RFP filter. Whole-cell recordings were performed using a MultiClamp 700A amplifier (Molecular Devices) and acquired using pClamp software (Clampex v.9.2, Molecular Devices). Data were sampled at 20 kHz and low-pass filtered at 1 kHz. Optogenetic stimulation of the virus-infected cells was done by shining fluorescent light through a 63x objective onto the slices using a GFP filter and pulsing the light with the help of a shutter driven via a Uniblitz VCM-D1 shutter (Vincent Associates) and a Master 8 pulse-generator (AMPI).

Behavioral test in a corridor. Locomotor behavior was recorded with the TSE MotoRater system (Belardita and Kiehn 2015). In short, mice were allowed to move spontaneously along a Plexiglas linear corridor while a high-speed camera (100-300 frames/s) filmed its movements from a bottom (transparent Plexiglas runway) and two side views (from either sides thought 2 mirrors oriented at 45 degrees with respect to the horizontal plane). Limbs were shaved and color markers were applied on the hip, knee, ankle and foot on both sides as described in (Caggiano et al., 2014). For each mouse, at least three trials where light stimulation was applied during ongoing locomotion were analyzed. In a separate series of experiments, four different acrylic obstacles (base: 4 cm width and 0.5 cm length) of increasing height (0.5, 1, 1.5, and 2 cm) were

placed in the middle of the runway at about 12 cm distance from each other (thus covering a length of about 50 cm on the runway). In this case, the camera was kept fixed in the obstacle area and videos were recorded at 100 frames/s.

Behavioral test in the open field. Open field test was conducted by placing the mice in a square Plexiglas box. The behavior was recorded by means of a ceiling mounted camera at 7.5 frames/s and motor activity extracted offline via Viewer 3 (Biobserve GmbH). Ambulation episodes were defined as periods when the animal moved more than 2 cm/s for at least 400 ms (3 frames). Control animals were *Chx10::Cre* littermates injected with equal volume (0.7 µL) of saline, bilaterally. Both groups (TeLC-injected and controls) were tested 3, 7, 9 or 14 days post-injection.

Data analysis of the single limb kinematic. Videos were analyzed using scripts written in Matlab (Mathworks Inc.) and R (www.r-project.org/). Motion capture of limb movements was reconstructed from the videos by semi-automatic tracking. The following angles were utilized for analysis: hip-foot angle, defined as the angle describing the extension and flexion (x-axis excursion) of the foot relative to the hip, the knee angle, the ankle angle and the foot angle. For the analysis of the kinematics, U-test or sign-rank test for circular data were used and a p-value of 0.05 was considered as threshold for significance. For the analysis of the open field behavior, averaged measures were obtained by bootstrapping and U-test or sign-rank test were used to compare population data. A p-value of 0.05 was considered as threshold for significance.

Gait analysis on the treadmill. Kinematics of mice running at different speeds where performed using a motorized treadmill (ExerGait-XL Treadmill for Gait Analysis, Columbus Instruments, USA). The ExerGait-XL treadmill system allows high-speed (100 frames/s) recording of animals' movements from a bottom-view while controlling the speed of a transparent belt on which mice run. Once habituated to run for 3 minutes to progressively higher speeds, animals were tested at different speeds from 5 to 20 m/min in bouts of 20 seconds with 1-2 minutes of inter-trials rest. Offline detection of paw ground-contact, i.e. stance and swing phases, was performed using TreadScan Software (TreadScan 4.0, Clever Sys, Reston, VA, USA). Standard gait parameters (including stride duration, stance, swing time) as well as homologue, left-right,

fore and hindlimb and diagonal coordinations were analyzed as previously described (Bellardita and Kiehn, 2015) via scripts written in Matlab (Mathworks Inc.) and R (www.r-project.org/).

Analysis of the locomotor behavior in presence of obstacles. Videos of animals running in the linear corridor in the presence of obstacles (see above) were analyzed offline. The position of the animal was extracted from the side view by means of background subtraction. Trajectories were filtered by means of a median filter with a window of 100 ms and stop events were considered when the animal reached a zero horizontal movement for at least 20 ms. Movements were analyzed for a maximum duration of 5 seconds. Image processing and data analysis were performed using scripts written in Matlab.

Area Under Receiver Operating Characteristic (AUROC) analysis. The distributions of probabilities of stop were compared for control versus TeLC treated-animals by their discernibility in 10 cm space before each obstacle. The distribution of controls was considered as true-positive and the TeLC treatment as true-negative. A Receiver Operating Characteristic curve was calculated as function of the probability of true positives from the probability of true negative. The Area Under the Receiver Operating Characteristic (AUROC) quantifies the distinction between the two distributions: a value close to 0.5 indicates that the two distributions are not different. Values toward 0 or 1 indicate a perfect discrimination between the two distributions. Statistical significance was calculated as in (Hanley and McNeil, 1982).

SUPPLEMENTAL REFERENCES

Arrenberg, A.B., Del Bene, F., and Baier, H. (2009). Optical control of zebrafish behavior with halorhodopsin. Proc Natl Acad Sci U S A *106*, 17968-17973.

Borgius, L., Restrepo, C.E., Leao, R.N., Saleh, N., and Kiehn, O. (2010). A transgenic mouse line for molecular genetic analysis of excitatory glutamatergic neurons. Mol Cell Neurosci *45*, 245-257.

Fuchs, A., Kutterer, S., Muhling, T., Duda, J., Schutz, B., Liss, B., Keller, B.U., and Roeper, J. (2013). Selective mitochondrial Ca2+ uptake deficit in disease endstage vulnerable motoneurons of the SOD1G93A mouse model of amyotrophic lateral sclerosis. J Physiol *591*, 2723-2745.

Hanley, J.A., and McNeil, B.J. (1982). The meaning and use of the area under a receiver operating characteristic (ROC) curve. Radiology *143*, 29-36.

Harrison, M., O'Brien, A., Adams, L., Cowin, G., Ruitenberg, M.J., Sengul, G., and Watson, C. (2013). Vertebral landmarks for the identification of spinal cord segments in the mouse. Neuroimage *68*, 22-29.

Kjaerulff, O., and Kiehn, O. (1996). Distribution of networks generating and coordinating locomotor activity in the neonatal rat spinal cord in vitro: a lesion study. J Neurosci *16*, 5777-5794.

Paxinos, G., and Franklin, K. (2001). The Mouse Brain in Stereotaxic Coordinates. San Diego: Academic Press *10.1111/j.1469-7580.2004.00264.x*.

Restrepo, C.E., Lundfald, L., Szabo, G., Erdelyi, F., Zeilhofer, H.U., Glover, J.C., and Kiehn, O. (2009). Transmitter-phenotypes of commissural interneurons in the lumbar spinal cord of newborn mice. J Comp Neurol *517*, 177-192.

Warp, E., Agarwal, G., Wyart, C., Friedmann, D., Oldfield, C.S., Conner, A., Del Bene, F., Arrenberg, A.B., Baier, H., and Isacoff, E.Y. (2012). Emergence of patterned activity in the developing zebrafish spinal cord. Curr Biol *22*, 93-102.